Alkali-metal-affected adsorption of CO on W(110) studied by metastable impact electron spectroscopy

W. Maus-Friedrichs, S. Dieckhoff and V. Kempter

Physikalisches Institut der TU Clausthal, W-3392 Clausthal-Zellerfeld, Germany

The adsorption of CO on clean and alkali-covered W(110) is studied by Metastable Impact Electron Spectroscopy (MIES) and UPS. Moleculary adsorbed CO is not observed for adsorption on clean W(110) neither by MIES nor by UPS at room temperature, but its existence cannot be excluded by the present results. From a comparison with data for the coadsorption of oxygen and K it is concluded that for K precoverages up to 0.8 ML features from the molecular adsorption of CO are seen in the MIE spectra. K precoverages beyond 0.8 ML, however, show spectral features corresponding to oxygen adsorption only. The exposure of a CO saturated W(110) surface to various amounts of K confirms that the complete disappearance of CO induced molecular spectral features occurs around 0.8 ML K coverage, and is mediated by a direct transfer of the K(4s) electron to the CO molecule.

1. Introduction

One of the most prominent systems for the investigation of coadsorption phenomena are CO and alkali metals. Surface science studies were concerned with the electronic, structural, vibrational, and energetic properties of the adsorbed species. The large electronic perturbation represented by an alkali atom adsorbed on a metal surface has also attracted the attention of theoreticians for many years. An excellent review of the status of alkali/CO coadsorption until 1988 is given by Bonzel [1].

Although MIES has already been applied to K/CO coadsorption on Ni(111) [2] a systematic study as for the oxidation of a Cs monolayer on Cu(110) [3] is not available yet. We prefer the acronym MIES rather than MDS for the reasons discussed in ref. [4].

At present the "best" model for the interaction of CO with alkali covered metal surfaces assumes [1]:

– direct interaction between the antibonding $2\pi^*$ orbital of CO and the s-state of the alkali metal;
– 5σ donation from the CO coadsorbate to the metal;

– back-donation from the metal into the antibonding $2\pi^*$ orbital.

The consequences of this model – as far as CO dissociation and adsorption are concerned – are the following: The CO adsorption energy increases due to the $4s/2\pi^*$ interaction in the presence of the alkali metal, and the C–O-bond becomes weaker facilitating CO dissociation. The bond energies of the atomic species C and O may increase. Whether coadsorption enhances molecular adsorption of CO depends upon details of the potential hypersurface of the CO/K–W(110) system.

MIES is ideally suited to detect changes of surface bond strengths as well as the weakening of bonds within molecular adsorbates. We have studied CO adsorption on W(110) precovered by alkali atoms, in particular K, by applying MIES, UPS and AES (for the determination of the alkali coverage). Electron energy spectra have been measured (1) as function of the CO exposure for various alkali precoverages in the range up to the completion of the first layer, and (2) as a function of alkali exposure to a W(110) surface saturated by CO.

Because a considerable fraction of the CO is dissociatively attached on clean and alkali pre-

covered W(110) the interpretation of the collected spectra demands for a solid understanding of the alkali–oxygen coadsorption on W(110). A detailed description of such studies will be given in a forthcoming paper [5], but some of the results will be used here. Moreover, a unique identification of some peak structures required UPS and MIES studies of alkali films with a thickness of more than 2 ML exposed to CO and oxygen.

The main finding of this work are:

- CO induced molecular features are neither detected by MIES nor by UPS for the adsorption of CO alone on W(110) at room temperature under the chosen conditions;
- CO induced molecular features can be detected in the presence of K atoms (up to about 0.8 ML K coverage);
- the coadsorbed K atoms weaken the molecular bond by direct transfer of the K(4s) electron to the CO molecule (most likely into the $2\pi^*$ orbital).

2. Experimental

The apparatus for performing combined MIES and UPS studies has been described before together with results for hydrogen/alkali coadsorption on W(110) [6]. Briefly, it consists of a cold cathode discharge capable of producing both metastable inert gas atoms and UV photons of the inert gas resonance lines. A pure UV photon beam is obtained when quenching the metastable atoms. When performing MIES measurements, the photoelectrons do not contribute significantly to the electron signal except beyond the maximum kinetic energy of 15.6 eV which corresponds to emission from the Fermi level induced by He(2^{1}S) atoms. The He beam contains both singlet and triplet metastable atoms. Our source is designed as in refs. [7,8] but modified for operation with an UHV system. According to ref. [8] the singlet/triplet ratio is about 1 : 7. No effort has been made so far to produce a pure triplet beam which can be achieved by optically pumping the 2^{1}S atoms into the 2^{1}P state.

The metastable current amounts to about 10^{10} He*/s or 2×10^9 Ne*/s with a diameter of about 1 mm on the target at a distance of 45 cm from the source. Metastable Ne has been used at some occasions because the Ne atom is much more sensitive for the ionization of p-derived orbitals of the target. The excitation energy amounts to 19.8 (20.6) eV for He*(2^{3}S) (He*(2^{1}S)) and 16.2 eV for Ne*(3^{3}P$_2$).

Alkali deposition is made using SAES Getters dispensers. The cleanness of the alkalated surface has been checked regularly by means of AES, work function measurements and MIES itself. No contamination of the alkali layer by CO, oxygen or water due to the dispenser could be observed.

Energy analysis was performed using a VSW hemispherical analyzer operated at constant pass energy with a resolution of about 250 meV.

Surface cleanness was routinely monitored by LEED, AES and work function measurements, but MIES itself represents the most sensitive technique for the detection of contamination due to the residual gas.

In all spectra shown below the metastables impinge upon the crystal under 45°. The energy analyzer also views the crystal under 45°. All results have been obtained with the crystal at room temperature (about 300 K). MIE spectra are presented as a function of the kinetic energy of the emitted electrons. Emission from the Fermi level ($E_B = 0$) corresponds to $E_{kin} = 16.2$ eV for UPS, $E_{kin} = 14.8$ (15.6) eV for He(2^{3}S) (He(2^{1}S)), and $E_{kin} = 12.2$ eV for Ne*(3^{3}P$_2$). In all spectra electrons with kinetic energies below 1 eV are suppressed. Therefore the change of the surface work function caused by the adsorption of alkali atoms and/or CO cannot be derived from our results.

UV spectra (see fig. 4a for an example) have been collected using the metastable beam source as UV source (see above). Its intensity is comparable to the commercial UV source available from VSW.

Results

Measurements have been taken in one of the following ways:

(1) W(110) has been precovered by the desired fraction of an alkali monolayer; the method for
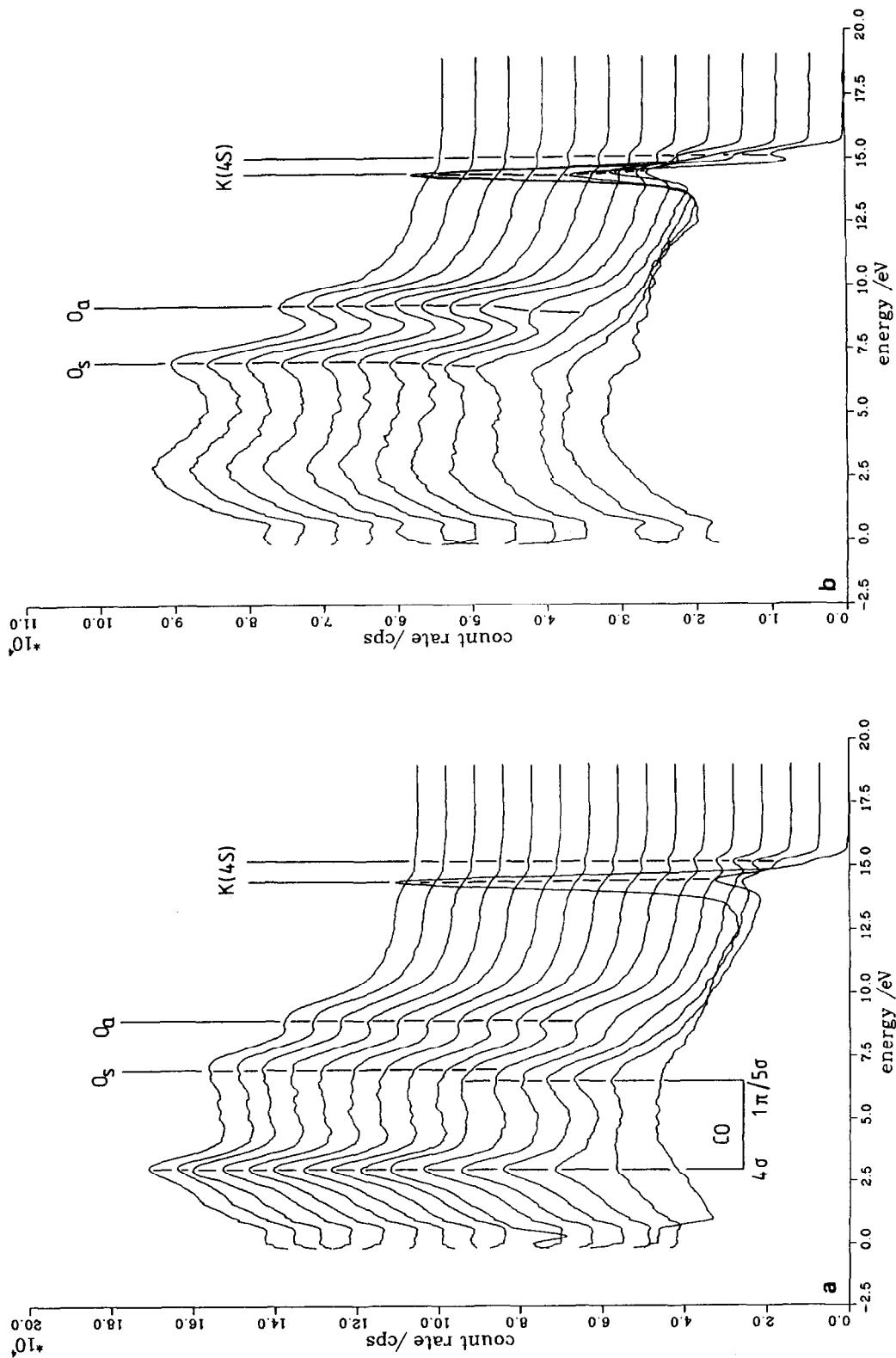
Fig. 1. MIE spectra of a W(110) surface precovered by 0.45 ML of potassium as a function of gas exposure. The bottom curve corresponds to 0 L. The exposure increases by (a) 0.25 L CO per spectrum, (b) 0.125 L O_2 per spectrum.
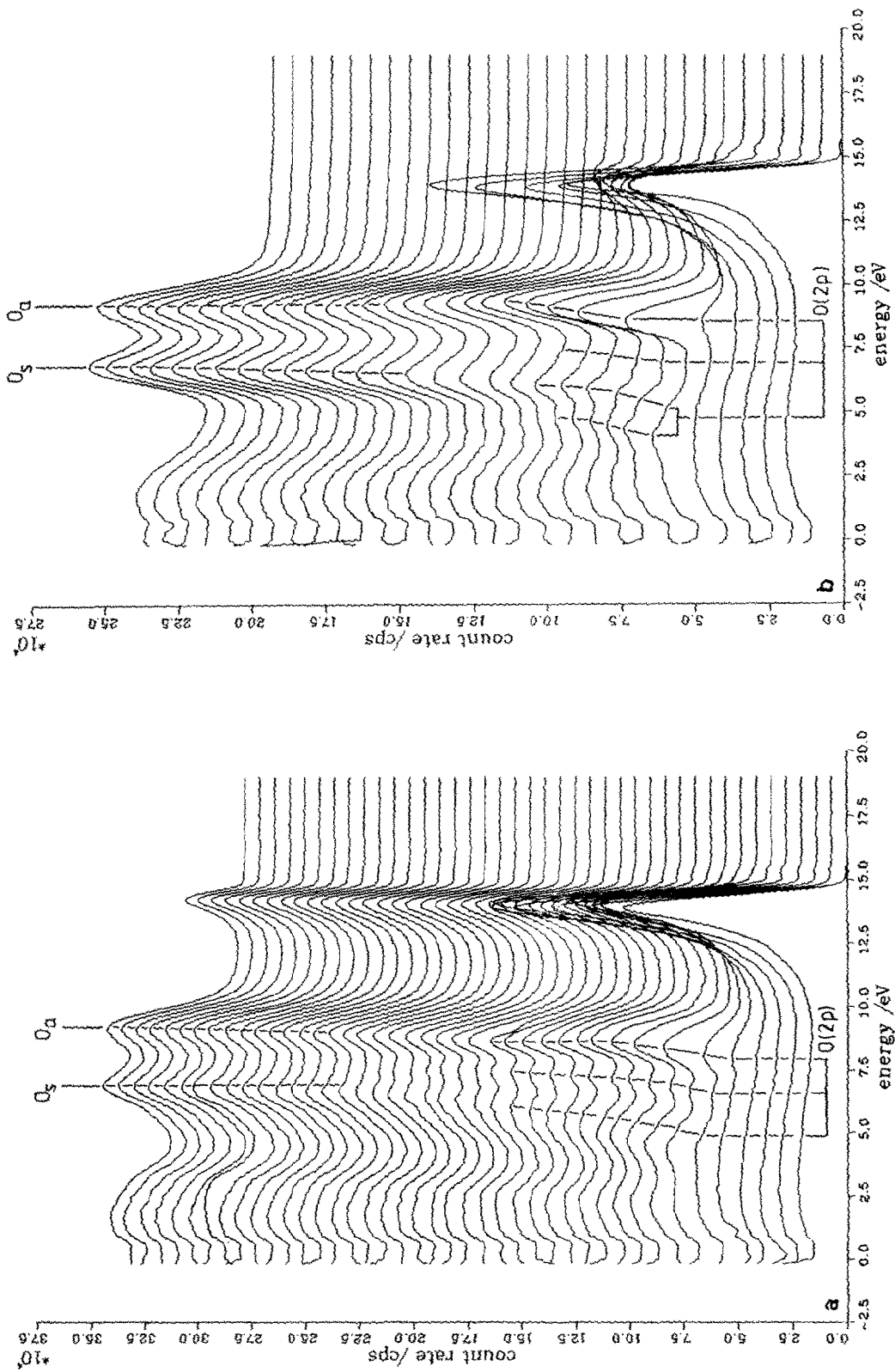
Fig. 2. MIE spectra of a W(110) surface precovered by 1.0 ML of potassium as a function of gas exposure. The bottom curve corresponds to 0 L. The exposure increases by (a) 0.25 L CO per spectrum, (b) 0.125 L O_2 per spectrum.
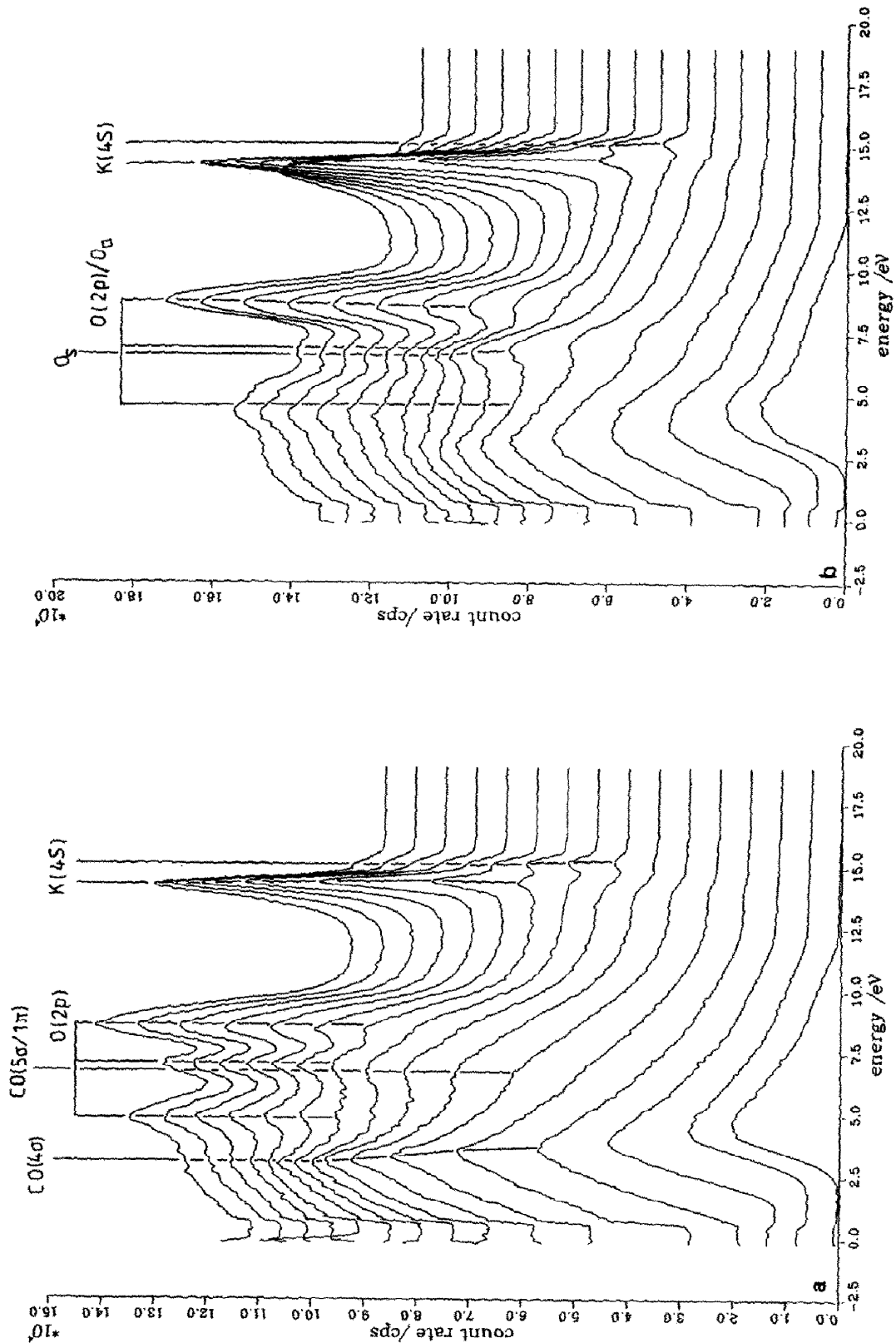
Fig. 3. MIE spectra of a W(110) surface saturated with 10 L gas as a function of exposure to potassium. The K coverage increases by about 0.09 ML. Bottom curve corresponds to the AN spectra obtained without K coadsorption. The precoverage is (a) 10 L CO, (b) 10 L O₂.

calibrating the coverage is described in ref. [6]. CO gas is admitted at a slow leak rate usually between 0.1 and 1 L CO per minute. Electron energy spectra are taken in regular time intervals, usually one per minute. The collection of a MIE spectrum and the storage of the data set requires about 50 s. UP spectra, however, need about 6 min data collection time using the MIES/UPS source. Figs. 4a and 4b show examples of the recorded raw spectra; all data displayed in figs. 1–3 were smoothed as indicated in fig. 4.

(2) After flashing the crystal to about 2400 K it is exposed to CO (after about 2 min) before cooling down completely to room temperature; typical exposures have been about 10 L CO at a pressure of about 5×10^{-8} Torr. Alkali atoms are then offered to the surface from a SAES Getters dis-

penser with a slow rate, usually about 0.1 ML per minute. Again the electron energy spectra are taken in regular time intervals of 1 min.

3.1. CO / W(110)

In general MIE spectra display contributions from two types of Auger processes, Resonance Ionization followed by Auger Neutralization (RI/AN) and Auger Deexcitation (AD). Which one of the Auger processes occurs is determined by the electronic state of the (adsorbate covered) surface. Clear discussions of this topic may be found in refs. [9,10–12]. MIE spectra typical for AN are found for clean metal surfaces and metal surfaces exposed to gases like O_2 and H_2 [5,6,11].

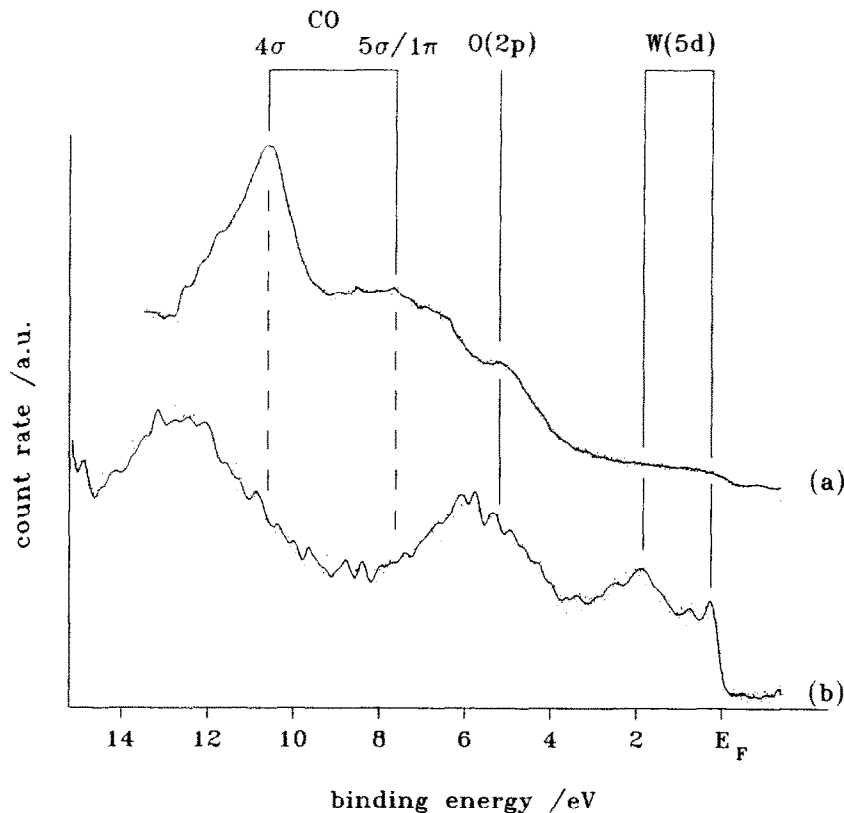Molecular adsorption of CO on Pd(111) and

Fig. 4. MIE spectra (a) and He I UP spectra (b) of a W(110) surface precovered by 0.49 ML K and saturated with CO (10 L).

Cu(110) has produced typical AD spectra which clearly display the two peaks from the ionization of the 4σ and $1\pi/5\sigma$ CO orbitals [9,13]. It was concluded that the molecularly adsorbed CO efficiently shields the metal surface thus inhibiting the RI/AN sequence.

The MIE spectra shown at the bottom of figs. 3a and 3b (CO(10 L)/W(110) and O_2(10 L)/W(110)) are typical examples for AN spectra. Similar spectra although much less degraded at small binding energies are also obtained for clean W(110) [6,11]. Investigations with He I UPS (not shown here, but with results similar to fig. 4b) for clean W(110) exposed to CO do also not show any feature which can be attributed to ionization of CO orbitals. One (or a combination) of the following reasons may be responsible for the absence of CO features in the spectra: (i) CO dissociates with high probability when adsorbing on clean W(110). It was already shown that under the conditions of our experiment (room temperature and low pressure adsorption) a large fraction of the CO is dissociated into the β-state on clean W(110) [14,15,16]. (ii) CO molecules are adsorbed in a manner that the RI/AN process is not inhibited because the metal is not shielded efficiently by the adsorbed molecule [10].

A decision will be attempted in section 4 on the basis of the results of section 3.3.

3.2. Coadsorption of CO on K/W(110)

Adsorption of K on W(110) produces a strong peak located near the Fermi energy (see figs. 1–3). This peak appears for the first time at a K coverage of 0.4 ML, and is due to the ionization of K(4s). The degree of coverage is given in fractions of the K saturation coverage on W(110) at room temperature. At 0.8 eV larger kinetic energy a satellite peak appears which is due to K(4s) ionization by the He($2\,^1$S) metastables also present in the beam. The transition from the AN spectrum for clean W(110) to the AD spectrum of the K-covered surface is very similar to that of Cs on W(110), and was already discussed in some detail in ref. [6].

Fig. 1a shows the MIE spectra obtained for the coadsorption of CO on a surface precovered by K

($\theta_K = 0.45$ ML). The CO exposure increases by 0.25 L CO per spectrum.

Fig. 1b shows the results for 0.45 ML K/W(110), but exposed to oxygen. From the comparison of figs. 1a and 1b we conclude that the peak at $E_B = 5.8$ eV ($E_{kin} = 9.0$ eV) (O_a) must be attributed to oxygen. The narrow peak at $E_B = 11.5$ eV (labeled 4σ CO) ($E_{kin} = 3.3$ eV) which is only seen for CO exposure appears at the position where 4σ CO ionization is commonly found in UPS. The feature centered around $E_B = 8$ eV (labeled $5\sigma/1\pi$ CO) ($E_{kin} = 6.8$ eV) appears where emission from the 5σ and 1π orbitals of CO is expected.

At larger exposures this latter peak is certainly a mixture of contributions from the CO($5\sigma/1\pi$) and (atomic) oxygen (O_s). It will be shown in ref. [5] (see also below) that the structures O_s and O_a are due to adsorption of atomic oxygen either on the substrate (s) or near a K atom (a). MIE spectra which also display similarly broad $5\sigma/1\pi$ features were reported by Rocker et al. [13] for the adsorption of CO on Ru(0001). The spectral features labelled 4σ and $5\sigma/1\pi$ CO are also seen when the CO saturated surface is subjected to small amounts of K (see fig. 3 and section 3.3).

Fig. 2a shows the results for the coadsorption of CO on a K-saturated ($\theta_K = 1$ ML) W(110) surface. The CO exposure increases by 0.25 L per spectrum. Fig. 2b shows the corresponding results obtained when exposing the K adlayer to molecular oxygen. The K(4s) emission disappears already completely for exposures > 1 L. However, the same spectral features as for CO exposure appear between $E_B = 5$ and 10 eV. This supports that (i) no molecular CO features are present in fig. 2a, and in turn, (ii) no features of molecular, but only of atomic oxygen appear in fig. 2b because dissociative attachment of CO should not lead to the formation of molecular oxygen.

In agreement with the peak assignment offered by Woratschek et al. [3] for the coadsorption of Cs and oxygen on Cu(110) and our measurements for the coadsorption of Cs or K and oxygen on W(110) [5] we assign the peaks seen between $E_B = 5.8$ and 10.0 eV to atomic oxygen: briefly, the three-peak-structure ($E_B = 5.8, 7.4, 9.7...10.3$ eV) ($E_{kin} = 9.0, 6.1, 5.1...4.5$ eV) seen for CO exposures < 2 L in

fig. 2a and for oxygen exposures < 1 L in fig. 2b is due to integration of atomic oxygen into the K adlayer. This structure can also be seen in figs. 3a and 3b for large K exposures to CO/W(110) and O_2/W(110), respectively. The two peaks dominating for CO exposures > 4 L are most likely due to atomic oxygen on top of the K atom ($E_B = 6.0$ eV, $E_{kin} = 8.8$ eV) and on the substrate ($E_B = 8.0$ eV, $E_{kin} = 6.8$ eV) [17]: the radius of a K atom shrinks considerably upon oxygenation [3] by about 30%, and absorption sites on the substrate become accesible with forthgoing oxygenation.

Results (not shown in fig. 2a) for exposures > 5 L show that even after the disappearance of the K(4s) emission there is still electron emission extending up to the Fermi level (see fig. 4a). Neither by MIES nor by UPS features due to C(2p) have been found. AES measurements show that at least some fraction of the C atoms from the CO dissociation is dissolved in the bulk.

Measurements similar to those of figs. 1 and 2 have also been performed for other K precoverages. Molecular features (at $E_B = 11.5$ and 8 eV) similar to those in fig. 1a are seen in the precoverage region $0.2 < \theta_K < 0.8$ ML.

The same molecular features at $E_B = 11.5$ and 8 eV are obtained when offereing CO to W(110) which was precovered by Li and Na in the submonolayer range up to 1 ML [23].

3.3. Coadsorption of K on CO / W(110)

Fig. 3a shows results for the coadsorption of potassium on a CO-saturated (10 L) W(110) surface. The K layer thickness increases by an amount corresponding to 0.09 ML per spectrum. As discussed previously the first spectrum ($\theta_K = 0$) is caused by AN. At K coverages around $\theta_K = 0.4$ ML the molecular features already familiar from fig. 1a can clearly be seen again. The peak labeled CO($5\sigma/1\pi$) may contain some contribution from O_s (see fig. 3b). Around 0.7 ML K the CO induced features start to weaken appreciably. Finally only the O(2p) derived peaks discussed with fig. 2 remain.

Fig. 3b shows the MIE spectra obtained for the coadsorption of potassium on the oxygen covered W(110) surface. At small K coverages peaks due

to AD of the He* at O atoms on the substrate (O_s at $E_B = 7.5$ eV) and near the K atoms (O_a at $E_B = 5.8$ eV) appear. The peak energies correspond to those of the structures seen in fig. 2 at large exposures. At large K coverages both for O_2 and CO three peaks characteristic for the integration of O atoms into the K adlayer remain visible.

Results with Ne* show the same features as the spectra of figs. 1–3; in general peaks occur at the same binding energies although their relative size in usually different from those found for He*. More importantly again no peak, but only a flat contribution from $2\pi^*$ occupation is found for this system near $E_B = 0$.

Qualitatively similar results have been obtained offering Li and Na to a W(110) surface precovered with 10 L CO [23].

3.4. Comparison of MIES and UPS for K / CO / W(110)

Fig. 4 compares the MIE (a) and UP (b) spectra of the W(110) surface covered by 0.49 ML K and saturated with CO (10 L). The spectra are aligned in such a way that the two Fermi energies coincide. Only the MIE spectrum clearly displays the CO induced feature labeled 4σ CO which, if present at all, can only weakly be seen in the UP spectrum. The broad shoulder (labeled $5\sigma/1\pi$ CO) is also not clearly apparent in the UP spectrum. Apart from the W(5d) emission the only prominent feature of the UP spectrum is the O(2p) emission at $E_B = 6$ eV (which is also evident in the MIE spectrum) The "rehybridization" model in ref. [18] states that a considerable change of the electronic structure of CO occurs upon interaction with coadsorbed K atoms. The absence of the peak labeled 4σ CO in the UP spectrum is thought to be due to the resulting change of the He I photoionization cross section. The rehybridization leads to a 1.5 eV splitting of the $5\sigma/1\pi$ composite peak [18]. The resulting flat structure between $E_B = 6$ eV and 8 eV cannot easily be distinguished from the strong O(2p) emission resulting from β-CO. We have also taken He I UP spectra under the conditions of figs. 1–3. In all cases CO-induced molecular features cannot be detected.

4. Interpretation

Figs. 1a and 3 present convincing evidence that the molecular features must be attributed to 4σ and $5\sigma/1\pi$ CO emission although the CO molecule may be distorted by the presence of the alkali coadsorbate. In particular we note that (i) always two additional CO induced features are observed, and their positions agree roughly with those known from UPS data for the 4σ and $5\sigma/1\pi$ CO emission; (ii) in particular the peak located at $E_a = 11.5$ eV cannot be identified with any known oxygen emission; (iii) additional experiments replacing K by Li and Na (not shown) display the same molecular features.

Both, the large binding energy and the wide peak from the 5σ and 1π emission (see figs. 1a and 2a) have been found in LDF calculations for the coadsorption of CO and K on Ni(001), but for a more dense K adlayer [19]. The calculations showed that the main effect of K coadsorption onto CO/Ni(001) is a shift of the molecular single-particle energies to larger binding energies with respect to E_F: the CO 4σ and 1π levels are shifted by 2 eV. Evidence for a direct interaction between the K(3p) electrons and the molecular 1π level is found which manifests itself in a pronounced broadening of the CO 1π orbital by about 2 eV. Both the unequal shift of 1π and 5σ and the bonding induced broadening of 1π are responsible for the broadening of the $1\pi/5\sigma$ feature to more than 2.0 eV for CO/K coadsorption.

As is evident from figs. 1 and 2 the K(4s) induced feature rapidly decreases upon CO adsorption; a direct interaction between the antibonding $2\pi^*$ orbital with the s-orbital of the alkali atom is thus likely [1]. For all CO exposures electron emission is observed up to the Fermi level: the results of Rocker et al. [13] show that the $2\pi^*$ states become partially occupied under K coadsorption. For CO and K on Ni(001) the calculations of Wimmer et al. [19] show a contribution due to $2\pi^*$ population extending 3 eV below E_F; the rise of the DOS right at E_F predicted for this system is not found by us for the CO/K–W(110) system.

It is generally believed that alkali coadsorption weakens the CO bond. From the appearance of molecular features after K coadsorption ($0.2 < \theta_K < 0.7$ ML) we must conclude that the absence of CO features in MIES in the case of CO/W(110) does not indicate complete CO dissociation. This indicates that the molecularly adsorbed CO is present at the surface in such a way that the RI/AN process is not suppressed in the case of CO/W(110). The reason for this fact may be the coexistence of atomic oxygen and CO on W(110): the oxygen induced enlargement of the work function could be resonsible for the dominance of the RI/AN over the AD process.

A one-dimensional potential diagram as described by Brodén et al. [20] and Ertl et al. [21] is a convenient way to visualize the adsorption/dissociation mechanism: there are two potential wells for dissociative and molecular CO adsorption is located closer to the surface (see fig. 21 of ref. [1]). For CO adsorption on clean W(110) the adsorption energy is small, and under stationary conditions there is dissociative adsorption mostly. The coadsorption of K and CO increases the CO adsorption energy due to the K(4s)/CO($2\pi^*$) interaction leading to partially ionic chemisorption. In the language of the potential diagram this implies that the potential well for molecular adsorption deepens in the presence of K atoms. On the other hand there is a larger occupation of the antibonding $2\pi^*$ levels than without K coadsorption which facilitates CO dissociation [1,21]. This means that the barrier between the two wells in the potential diagram becomes lower, and its width may decrease. The bond energy of the atomic oxygen does not change much upon K coadsorption as judged from MIES results.

Our results suggest that K – although enlarging the adsorption energy of CO – weakens the (C–O)-bond, e.g., lowers the barrier between the two potentials and thus leads to an enhanced rate for CO dissociation and atomic adsorption on W(110) at room temperature. It should be kept in mind that a one-dimensional potential diagram is an extremely simplified visualization of the reaction coordinate representing a complicated cut through the potential hypersurface of our system.

5. Summary

A study of the coadsorption of CO and K on W(110) with UPS and metastable impact electron spectroscopy (MIES) is presented. Below a K precoverage of 0.2 ML no CO induced features are observable in MIES and UPS. In the range of K-precoverages between 0.2 and 0.8 ML some fraction of the coadsorbed CO is adsorbed molecularly as detected by MIES; this is concluded from the appearance of two CO induced features at the binding energies $E_B = 11.5$ and 8 eV. Dissociatively coadsorbed CO gives spectral features which can be identified as being caused by adsorption of atomic oxygen. In the coverage range from 0.2 to 0.8 ML molecularly and dissociatively attached CO coexist. Beyond 0.8 ML K precoverage coadsorbed CO is dissociated completely for any studied CO exposure. The coadsorption of K on the CO precovered surface induces the same molecular features as discussed above provided the K coverage remains below approximately 0.8 ML. There is evidence that some molecularly adsorbed CO is present even on the clean surface in a way that the Resonance Ionization/Auger Neutralization process in MIES is not suppressed.

Acknowlegdments

References

[1] H.P. Bonzel, Surf. Sci. Rep. 8 (1988) 43.
[2] J. Lee, C.P. Hanrahan, J. Arias, R.M. Martin and H. Metiu, Phys. Rev. Lett. 51 (1983) 1803.
[3] B. Woratschek, W. Sesselmann, J. Küppers, G. Ertl and H. Haberland, J. Chem. Phys. 86 (1987) 2411.
[4] W. Keller, H. Morgner and W.A. Müller, Mol. Phys. 58 (1986) 1039.
[5] W. Maus-Friedrichs, S. Dieckhoff, M. Wehrhahn and V. Kempter, to be published.
[6] W. Maus-Friedrichs, M. Wehrhahn, S. Dieckhoff and V. Kempter, Surf. Sci. 237 (1990) 257.
[7] O. Leisin, H. Morgner and W. Müller, Z. Phys. A 304 (1982) 23.
[8] H. Hotop, E. Kolb and J. Lorenzen, J. Electron Spectrosc. Relat Phenom. 16 (1979) 213.
[9] W. Sesselmann, B. Woratschek, G. Ertl, J. Küppers and H. Haberland, Surf. Sci. 146 (1984) 17.
[10] G. Ertl, J. Küppers, Low Energy Electrons and Surface Chemistry, 2nd ed. (VCH, Weinheim, 1985).
[11] W. Sesselmann, B. Woratschek, J. Küppers, G. Ertl and H. Haberland, Phys. Rev. B 35 (1987) 8348.
[12] H.D. Hagstrum, Springer Ser. Surf. Sci. 10 (1988) 341
[13] G. Rocker, H. Tochihara, R.M. Martin and H. Metiu, Surf. Sci. 181 (1987) 509.
[14] E. Umbach, J.C. Fuggle and D. Menzel, J. Electron Spectrosc. Relat. Phenom. 10 (1977) 15.
[15] E. Umbach, D. Menzel, Surf. Sci. 135 (1983) 199.
[16] E. Umbach, Doctoral Thesis, München (1980).
[17] E.G. Michel, J.E. Ortega, E.M. Oellig, M.C. Asensio, J. Ferrón and R. Miranda, Phys. Rev. B 38 (1988) 13399.
[18] J.J. Weimer and E. Umbach, Phys. Rev. B 30 (1984) 4863.
[19] E. Wimmer, C.L. Fu and A.J. Freeman, Phys. Rev. Lett. 55 (1985) 2618.
[20] G. Brodén, G. Gafner and H.P. Bonzel, Surf. Sci. 84 (1979) 295.
[21] G. Ertl, M. Weiss and S.B. Lee, Chem. Phys. Lett. 60 (1979) 391.
[22] F.P. Netzer, D.L. Doering and T.E. Madey, Surf. Sci. 143 (1984) L363.
[23] W. Maus-Friedrichs, Doctoral Thesis, Clausthal (1991).